Discovery of boron-conjugated 4-anilinoquinazoline as a prolonged inhibitor of EGFR tyrosine kinase†

Hyun Seung Ban,[a] Taikou Usui,[a] Wataru Nabeyama,[a] Hidetoshi Morita,[b] Kaori Fukuzawa[c] and Hiroyuki Nakamura*[a]

Received 14th May 2009, Accepted 15th July 2009
First published as an Advance Article on the web 20th August 2009
DOI: 10.1039/b909504g

Boron-conjugated 4-anilinoquinazolines were designed and synthesized as inhibitors of EGFR tyrosine kinase with possible covalent bond interactions between the boron atom and the nucleophilic groups of the EGFR kinase domain. Among the compounds synthesized, compounds **6c**, **7b**, and **7d** reduced the EGF-mediated phosphorylation of EGFR tyrosine kinase and its downstream kinases including ERK and Akt in A431 cells. The cell growth was inhibited by these compounds through arrest of G1 cell cycle, which induced apoptosis. A time-dependent *in vitro* preincubation assay demonstrated the irreversible inhibition of compound **7d** against EGFR tyrosine kinase. Quantum mechanical docking simulation revealed that the boronic acid moiety of compound **7d** formed a covalent B–O bond with Asp800 in addition to hydrogen bonds with Asp800 and Cys797, which may cause the prolonged inhibition of compound **7d** toward EGFR tyrosine kinase.

Introduction

The signal transduction pathway through growth factor receptor tyrosine kinases is important for cell proliferation. Deregulation of signaling pathway has been observed in many human tumors, and thus these kinases have been investigated as potential targets for cancer therapy.[1] Epidermal growth factor receptor (EGFR) (also known as erb-B1 or Her-1) is a member of ErbB family of receptor tyrosine kinases, and the uncontrolled activation of EGFR-mediated signaling may be due to overexpression of the receptors in numerous tumors including head and neck, lung, breast, bladder, prostate, and kidney cancers, mutations resulting in constitutive activation in brain tumors, or overexpression of the ligands including EGF or TGF-α in pancreatic, prostate, lung, ovary, and colon cancers.[2,3]

In 1994, Fry and co-workers discovered 4-anilinoquinazoline (PD 153035) as a specific inhibitor toward EGFR tyrosine kinase.[4] Since their discovery, various 4-anilinoquinazoline derivatives have been synthesized, and ZD-1839 (Iressa™),[5,6] and OSI-774 (Tarceva™)[7,8] have been developed as reversible binding inhibitors of EGFR kinase activity and recently approved for non-small-cell lung cancer (NSCLC) therapy. Furthermore, Lapatinib has been investigated as a dual reversible ErbB inhibitor with potent activity against EGFR and Her-2 kinases, and approved for breast cancer therapy.[9,10]

However, despite the benefits of Iressa and Tarceva for treatment of NSCLC, most recurrent patients ultimately develop acquired resistance to these agents. Recently, a mutation, T790M, within the EGFR kinase domain has been found in ~50% of these patients, and therefore much attention has been paid for potency of irreversible EGFR inhibitors, which have proven to be effective for the EGFR tyrosine kinase with T790M mutation.[11,12] Among the various 4-anilinoquinazoline derivatives synthesized,[13–15] EKB-569 (phase II),[16,17] HKI-272 (phase I),[18] and CI-1033 (phase I)[19,20] have been investigated as irreversible inhibitors. These compounds have a Michael acceptor function, as a common structure, substituted at the 6-position of the quinazoline ring to trap the Cys-797 (Cys773 in an alternative numbering scheme) of EGFR, which may cause the irreversible inhibition. According to X-ray structural analysis of a complex with Tarceva, the thiol of Cys-797 in fact is located near the methoxyethoxy group substituted at the 6-position of Tarceva,[21,22] as shown in Fig. 1.

We focused on the substituent at the 6-position and designed boron-conjugated 4-anilinoquinazolines. A boron atom has a vacant orbital and interconverts with ease between the neutral sp^2 and the anionic sp^3 hybridization states, which generates a new stable interaction between a boron atom and a donor molecule through a covalent bond. Recently the X-ray crystal structure of the 20S proteasome in complex with bortezomib was reported.[23] In this structure, boronic acid of bortezomib covalently interacts with the Thr-1 hydroxyl in the active site of the 20S proteasome, forming the hybridized borate. Bond energies of C–S, B–S, and B–O σ-bonds have been estimated as 65, 24, and 18 kcal/mol, respectively,[24,25] and that of hydrogen bonding is 3–10 kcal/mol.[24,26] Therefore, if we can introduce a boron atom into the 6-position of the quinazoline framework *via* a linker of suitable length, as illustrated in Fig. 1A, a covalent bond interaction would be expected between the boron atom and the thiol of Cys797 or the carboxyl group of Asp800. This interaction, which is stronger than the hydrogen bond but not as strong as the

[a]*Department of Chemistry, Faculty of Science, Gakushuin University, Tokyo, 171-8588, Japan. E-mail: hiroyuki.nakamura@gakushuin.ac.jp; Fax: (+81)3-5992-1029; Tel: (+81)3-3986-0221*
[b]*Graduate School of Science and Engineering, Yamagata University, Yamagata, 990-8560, Japan*
[c]*Mizuho Information & Research Institute, Inc., Tokyo, 101-8443, Japan*

† Electronic supplementary information (ESI) available: QM/MM-optimized geometries for the docking mode of EGFR-compound **7d**, effects of ATP concentration on *in vitro* preincubation time-dependent EGFR inhibition by compound **7d**, and ^{1}H NMR spectra for compounds **2**–**4**. See DOI: 10.1039/b909504g

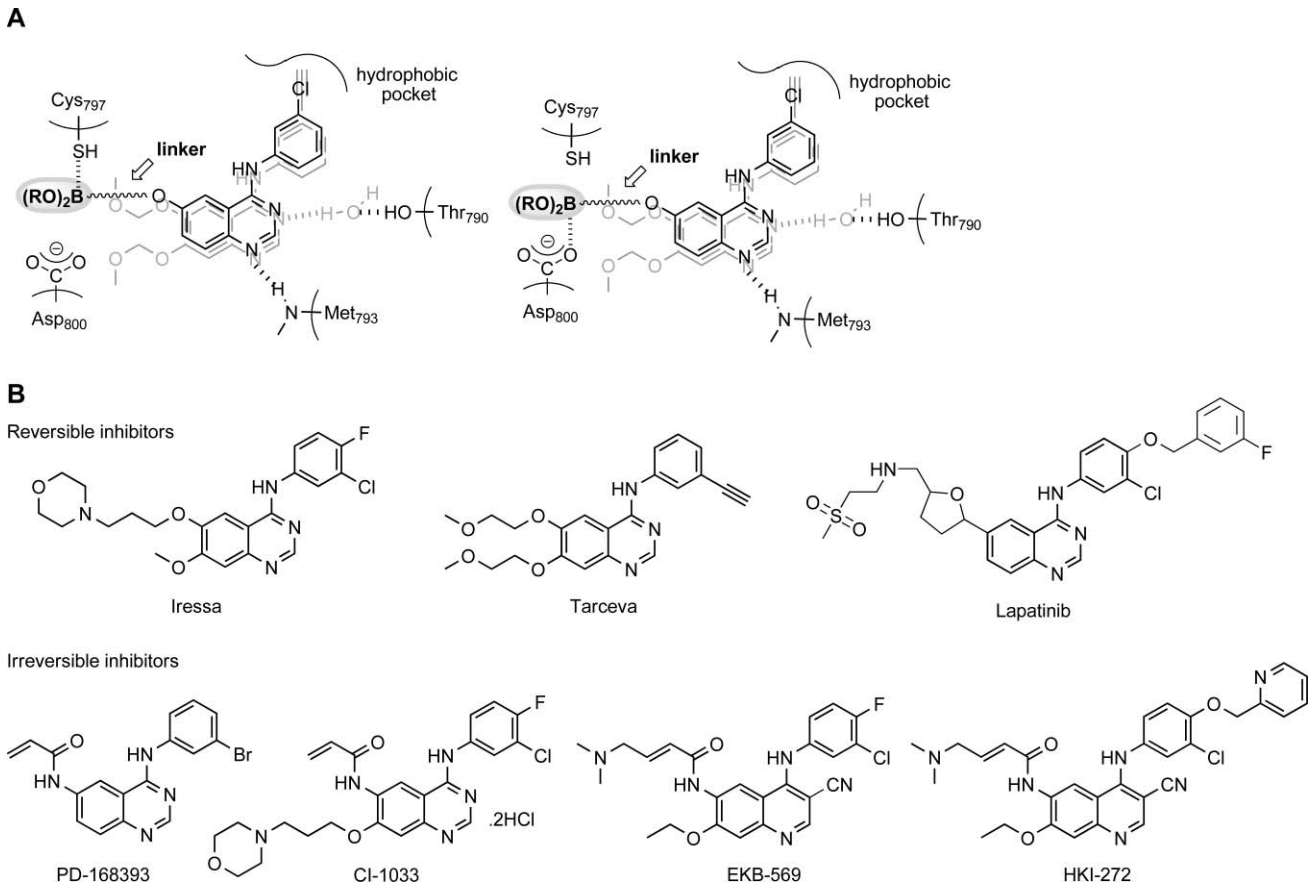

Fig. 1 (A) Expected binding conformation of boron-conjugated quinazolines (black) based on the X-ray crystal structure of the EGFR kinase domain in complex with Tarceva (gray, PDB code: 1M17). (B) Structures of reversible and irreversible inhibitors of EGFR tyrosine kinase.

C–S or C–O covalent bond,[27] may affect the prolonged inhibition of EGF-stimulated signal transduction.

In this paper, we have introduced a boron moiety into the anilinoquinazoline framework *via* various lengths of linkers, such as methylene (1.68 Å), propenyl (3.90 Å), and benzyl (5.81 Å) groups (Fig. 2). We synthesized various boron-conjugated 4-anilinoquinazolines and investigated their selective inhibition of EGFR kinase, inhibition of the EGFR-stimulated signaling pathway, and effects on cancer cell growth and cell cycle, as well as their irreversible interaction properties.

Furthermore, in order to analyze the EGFR-inhibitor binding forms and their interactions in detail, molecular simulations were carried out based on quantum mechanical (QM) methods. Classical molecular mechanical (MM) approaches based on an empirical force field have been widely used for molecular simulations of protein properties such as enzyme–inhibitor interactions. However, such an approach is not sufficiently accurate in the description of the nature of the interactions between molecules. Also, the force field of sp^3-hybridized boron atom has still not been established. On the other hand, a QM approach based on *ab initio* molecular orbital (MO) calculations has been successfully used to understand the structure and chemical properties of molecules including coordinate linkages of sp^3-hybridized boron atoms, and therefore the QM approach has potential for accurate representation of molecular interactions that could aid drug design.[28] Here, we have investigated docking geometries between the EGFR and inhibitor by hybrid QM/MM calculations in the ONIOM scheme,[29,30] employing a Hartree–Fock (HF) method for the QM part and a UFF force field for the MM part. Binding energies between the EGFR and inhibitors were also evaluated by full QM treatment using *ab initio* fragment molecular orbital (FMO) methods[31–34] at the HF level. This FMO approach has been successfully used to evaluate molecular interactions of biomacromolecules such as a binding affinity of ligands to the human estrogen receptor.[35,36]

Results and discussion

Chemistry

The synthesis of the boron-conjugated anilinoquinazolines **6a–d** and **7b–d** is shown in Fig. 2. Briefly, 5-hydroxyanthranilic acid **1** was converted to the quinazolinone **2** in 70% yield in three steps according to the reported procedure.[37] Protection of the hydroxy group of **2** with acetic anhydride gave the 6-acetoxyquinazoline **3**, which underwent chlorination with $POCl_3$ to give the 4-chloroquinazoline **4** in 66% yield. Displacement of **4** with 3-chloroaniline followed by deprotection of the acetyl group afforded the 6-hydroxy-4-anilinoquinazoline **5**, quantitatively.[38] Various boronic ester groups, such as $(RO)_2BCH{=}CHCH_2Cl$ (**8** and **9**), $(RO)_2BCH_2Br$ (**10**),[39] and $(RO)_2BC_6H_4CH_2Br$ (**13**), were synthesized and introduced into the 6-position of the

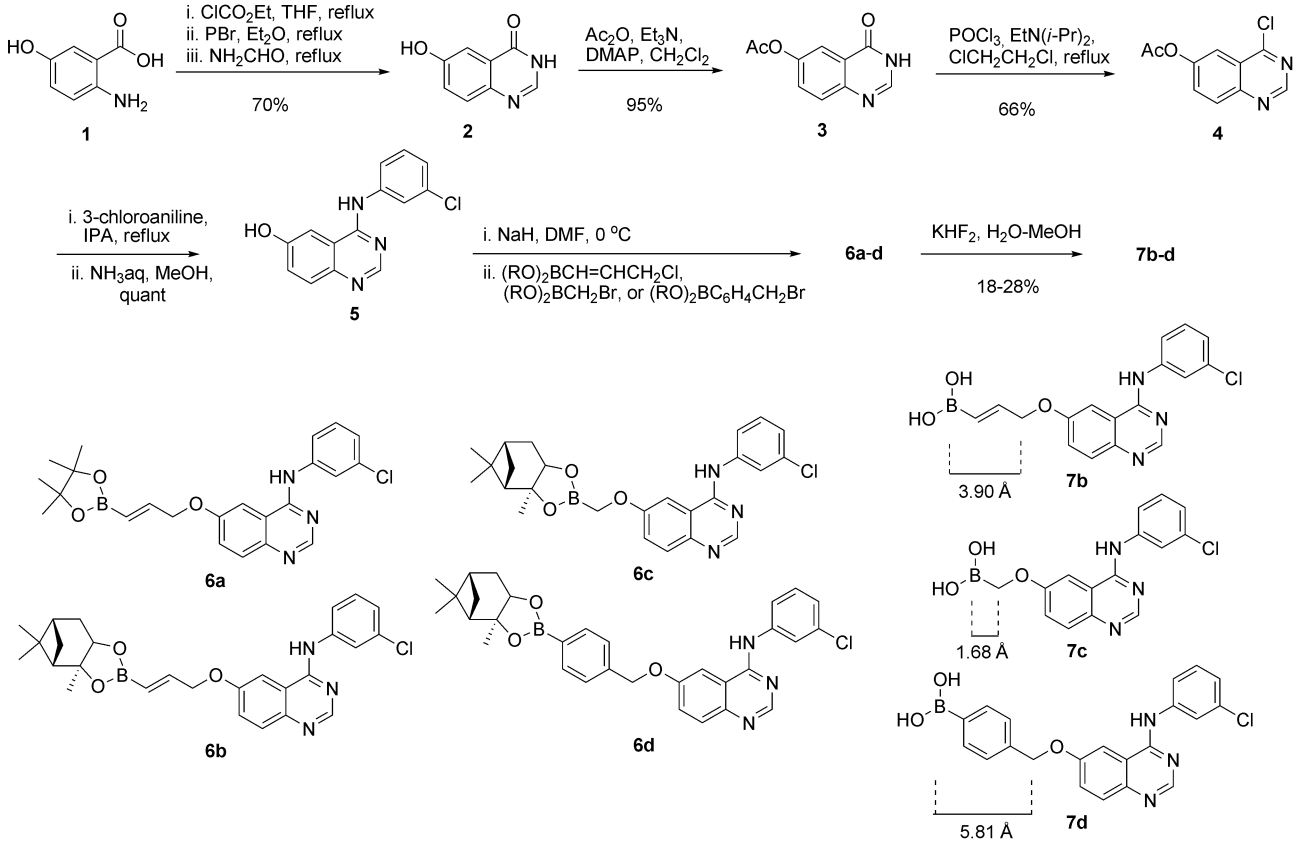

Fig. 2 Synthesis of boron-conjugated 4-anilinoquinazolines.

anilinoquinazoline **5** through ether bond formation to give the corresponding anilinoquinazolines **6a–d** in 7–51% yields. Deprotection of boronic esters **6a–d** was carried out by using KHF_2 in aqueous methanol to give the boronic acids **7b–d** in 18–28% yields.[40]

Enzyme and cellular inhibitory activities

Inhibitory activity of the boron-conjugated 4-anilinoquinazolines against EGFR, HER-2, Flt-1, and KDR tyrosine kinases, was determined by measuring the levels of phosphorylation of the tyrosine kinase-specific peptides *in vitro*.[41] As shown in Table 1, most of the boron-containing 4-anilinoquinazolines selectively suppressed EGFR tyrosine kinase activity without inhibiting HER-2, Flt-1 or KDR kinases, and their IC_{50} values against EGFR tyrosine kinase were lower than 1 μM. These results indicate that the conjugation of a boron moiety to the 6-position of 4-anilinoquinazolines has a selective inhibitory activity toward EGFR tyrosine kinase. Under our experimental conditions, Tarceva, which was used as a positive control for enzyme assay, also showed significant inhibition of EGFR tyrosine kinase (Table 1). Among the boron-conjugated 4-anilinoquinazolines synthesized, compounds **6d** and **7c** showed weak inhibitions of EGFR tyrosine kinase (20 and 45%, respectively) at 1 μM. Boronic acids **7b** and **7d** showed more potent inhibition compared to their ester derivatives **6a**, **6a**, and **6d**. Since the boron moiety may be located in the hydrophilic region surrounded by Cys797 and Asp800 in the binding formation to EGFR kinase, the boronic acids are preferable to the corresponding boron esters due to their steric and hydrophilic properties. In contrast, boronic acid **7c** showed less potent inhibition because the linker between the boronic acid and the quinazoline ring may be too short to occupy the hydrophilic region.

Table 1 Effects of the boron-conjugated 4-anilinoquinazolines on tyrosine kinase activity of EGFR, HER2, Flt-1, and KDR[a]

Compound	Inhibition at 1 μM (%)/IC_{50} (μM)[a]			
	EGFR	HER2	Flt-1	KDR
6a	55/0.64 ± 0.02	—/nd	—/nd	11/nd
6b	53/0.58 ± 0.01	—/nd	—/nd	6/nd
6c	65/0.20 ± 0.02	—/nd	—/nd	—/nd
6d	20/nd	—/nd	—/nd	—/nd
7b	63/0.27 ± 0.02	—/nd	—/nd	—/nd
7c	45/nd	—/nd	—/nd	—/nd
7d	55/0.85 ± 0.03	—/nd	—/nd	—/nd
Tarceva	82/0.06 ± 0.07	—/nd	—/nd	40/nd

[a] The drug concentrations are those required to inhibit the phosphorylation of the poly(Glu:Tyr) substrate by 50% (IC_{50}). They were determined from semilogarithmic dose–response plots, and represent the mean ± s.d. of triplicate samples. —, no inhibitory effect at 1 μM; nd, not determined.

We next examined the effects of the boron-conjugated 4-anilinoquinazolines on the EGF-induced tyrosine phosphorylation of EGFR and the signaling cascades in A431 cells by immunoblot analysis. Treatment of A431 with EGF (10 ng/ml) rapidly induced autophosphorylation of EGFR, and the level of the phosphorylation reached a maximum at 10 min after EGF

stimulation (data not shown). Under these conditions, the boron-conjugated 4-anilinoquinazolines potently suppressed the EGF-induced phosphorylation of EGFR at 1 μM concentration of compounds (Fig. 3A).

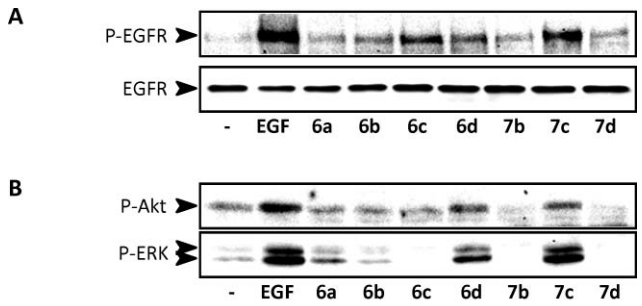

C

Compounds	GI_{50} (μM)			
	A431	SKBr3	KatoIII	HepG2
6a	1.31±0.16	9.39±0.22	>10	>10
6b	0.82±0.04	8.65±0.02	9.21±0.03	>10
6c	0.54±0.04	8.36±0.08	6.21±0.14	>10
6d	2.59±0.16	8.05±0.12	>10	>10
7b	0.68±0.02	7.81±0.31	7.45±0.02	>10
7c	1.30±0.09	7.36±0.10	6.29±0.02	>10
7d	1.82±0.02	8.45±0.06	6.80±0.13	>10
Tarceva	0.19±0.02	6.12±0.05	5.88±0.03	5.02±0.18

Fig. 3 Inhibition of the EGF-induced phosphorylation of EGFR and its downstream kinases, and cell growth. (A) and (B) A431 cells were incubated with the boron-conjugated 4-anilinoquinazolines (1 μM) or Tarceva (0.3 μM) and then stimulated with EGF (10 ng/mL). The levels of each kinase were detected by immunoblot analysis with the specific antibody. (C) A431, HepG2, KatoIII, or SKBR3 cells were incubated for 72 h with various concentrations (10 nM to 10 μM) of compounds and then the rates of viable cells were determined by MTT assay. The drug concentration required to inhibit cell growth by 50% (GI_{50}) was determined from semilogarithmic dose–response plots, and results represent the mean ± s.d. of triplicate samples.

It has been reported that the autophosphorylation of EGFR tyrosine kinase activated various downstream kinases including ERK and Akt, which play an important role in the regulation of cell proliferation and apoptosis, respectively.[42] Therefore, we examined the effects on the EGFR-dependent activation of downstream signaling pathways. As shown in Fig. 3B, the boron-conjugated 4-anilinoquinazolines, except compounds **6d** and **7c**, also significantly suppressed the EGF-induced phosphorylation of ERK and Akt in parallel with the inhibition of EGFR autophosphorylation. These results indicate that the boron-conjugated 4-anilinoquinazolines also induce the inhibitory effect on autophosphorylation of EGFR tyrosine kinase in cells as well as EGFR kinase *in vitro*, and arrest the downstream signaling pathway.

To demonstrate whether the inhibitory activity of the boron-conjugated 4-anilinoquinazolines toward EGFR tyrosine kinase is implicated in cell growth, we examined the effects of the compounds on proliferation of various human carcinoma cell lines (A431, HepG2, KatoIII, and SKBR3). The cells were incubated with compounds at various concentrations for 72 h and their cell growth inhibition was determined by MTT assay. As shown in Fig. 3C, the boron compounds reduced the proliferation of A431 cells, which overexpress EGFR, and their GI_{50} values were in the range 0.54–2.59 μM. Lower cell growth inhibitions were observed in other cell lines, which express a low level of EGFR. These results indicate that the selective inhibition of A431 cell growth by the boron-conjugated 4-anilinoquinazolines is a consequence of the inhibition of EGFR tyrosine kinase.

Cell cycle G1 arrest and induction of apoptosis

To characterize the cell growth inhibition induced by the boron-conjugated 4-anilinoquinazolines, effects of compounds on cell cycle were investigated by flow cytometry analysis. Treatment of A431 cells with compounds **6c**, **7b**, and **7d** at 1 μM for 24 h led to profound changes in cell-cycle profiles as shown in Fig. 4A. The boron-conjugated 4-anilinoquinazolines induced a massive accumulation of cells in the G1 phase and decreased the proportion of cells in G2/M phase. Tarceva also induced G1-arrest with a similar potency. To further characterize the cell-death mechanism induced by the boron-conjugated 4-anilinoquinazolines, a biparametric cytofluorimetric analysis was performed using FITC-labeled annexin V and propidium iodide (PI), which stain phosphatidylserine residue and DNA, respectively.[43] A431 cells

A

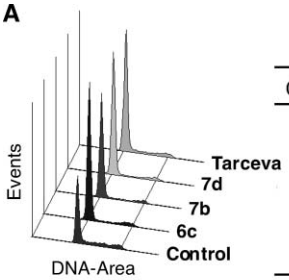

Compounds	G1	S	G2/M
Control	64.0%	5.4%	30.1%
6c	86.1%	3.0%	10.8%
7b	87.1%	3.8%	9.0%
7d	81.5%	4.0%	14.4%
Tarceva	89.7%	3.3%	7.0%

B

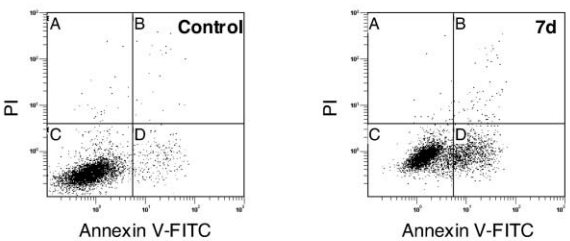

Compounds	A	B	C	D
Control	0.5%	0.5%	94.5%	4.5%
6c	0.2%	0.7%	79.3%	19.7%
7b	0.5%	1.0%	84.0%	14.5%
7d	0.3%	1.6%	77.0%	21.1%
Tarceva	0.3%	1.4%	75.0%	23.3%

Fig. 4 Induction of cell cycle G1 arrest and apoptosis. A431 cells were incubated for 24 h with the boron-conjugated 4-anilinoquinazolines (1 μM) or Tarceva (0.3 μM). (A) The cells were harvested and stained with propidium iodide (PI). (B) The cells were stained with annexin V-FITC and PI. The cell cycles and apoptosis were determined by a flow cytometer.

were treated with the compounds for 24 h and then stained with PI and FITC-labeled annexin V. The resulting green (FITC) and red (PI) fluorescence was monitored by flow cytometry. As indicated in Fig. 4B, the number of annexin V-positive and PI-negative cells increased by the treatment with compounds **6c**, **7b**, **7d**, and Tarceva (the area labelled D). These results indicate that the boron-conjugated 4-anilinoquinazolines possess not only antiproliferative but also apoptotic activities in the A431 cell growth inhibition through the suppression of EGFR tyrosine kinase activity.

Prolonged inhibition by irreversible binding to EGFR tyrosine kinase in cells

The prolonged inhibition ability of the boron-conjugated 4-anilinoquinazolines toward EGFR tyrosine kinase was investigated by experiment using A431 exposed to the compounds and washed prior to the assay.[15] After continuous incubation of A431 cells with the boron-conjugated 4-anilinoquinazolines at 1 μM or Tarceva at 0.3 μM for 1 h followed by EGF stimulation, each compound inhibited autophosphorylation of EGFR in A431 cells, as shown by immunoblot analysis (Fig. 5A). When the cells were washed to remove unbound compounds from the cell-medium and incubated for an additional 5 h prior to EGF stimulation, the activity of EGFR autophosphorylation was restored, while for cells treated with compound **7d**, the autophosphorylation was still inhibited. These results suggest that compound **7d** irreversibly inhibited to EGFR tyrosine kinase, whereas other compounds, such as **6c**, **7b**, and Tarceva, reversibly interacted to EGFR tyrosine kinase. Furthermore, the preincubation time-dependent inhibition of compound **7d** against the EGF-induced phosphorylation of EGFR was observed in A431 cells (Fig. 5B). These results also support the irreversible inhibitory property of compound **7d**. We next investigated the prolonged inhibition implicated in continuous reduction of cell growth. As shown in Fig. 5C, MTT assay revealed that compound **7d** showed retentive reduction of cell growth after removal of compounds from the cell-medium by washing even though its inhibitory activity was not potentially high in comparison with other compounds, whereas the inhibitory effects of other compounds including Tarceva were essentially lost upon washing. These results indicate that continued reduction of cell growth by compound **7d** may be due to the irreversible inhibition of EGFR tyrosine kinase. Fig. 5D shows dose-dependent growth inhibition curves of cells treated with compound **7d** with and without washing, and similar values for GI_{50} were observed in both cases. It was reported that the lack of autophosphorylation sites resulted in reduction of internalization and degradation rates of EGFR.[44] Therefore, the irreversible inhibition of EGFR autophosphorylation by compound **7d** induces prolonged reduction effects of internalization and degradation rates of EGFR, which may lead to the retentive reduction of cell growth.

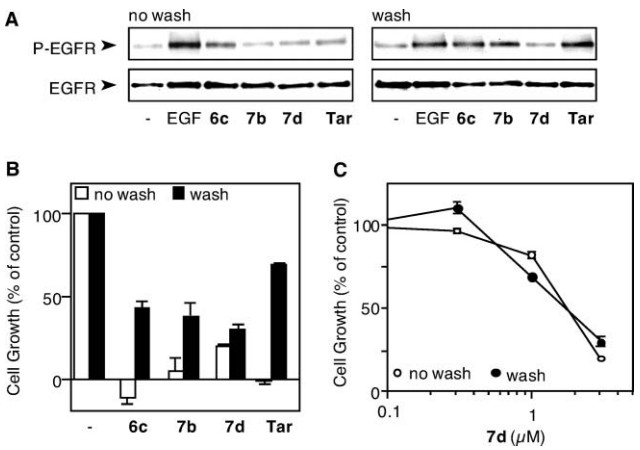

Fig. 5 Inhibition of the EGF-induced phosphorylation of EGFR and cell growth. (A) A431 cells were incubated with the boron-conjugated 4-anilinoquinazolines (1 μM) or Tarceva (Tar, 0.3 μM), and then stimulated with EGF (10 ng/mL) or washed with fresh medium for 5 h prior to stimulation of EGF. The levels of each kinase were detected by immunoblot analysis with the specific antibody. (B) Time-dependent inhibition of EGF-induced phosphorylation of EGFR by compound **7d**. A431 cells were incubated with the indicated time and concentration of compound **7d**, and then stimulated with EGF (10 ng/mL). (C) A431 cells were incubated for 18 h with compounds **6c** (1 μM), **7b** (1 μM), **7d** (3 μM) or Tarceva (0.3 μM) and then washed with fresh medium. After further incubation for 54 h, the rates of viable cells were determined by MTT assay. (D) Dose-dependent cell growth with or without wash of cells treated with compound **7d** was determined.

In vitro irreversible inhibition of EGFR tyrosine kinase activity

To clarify the irreversible inhibition of EGFR tyrosine kinase by the boron-conjugated 4-anilinoquinazoline in detail, *in vitro* time-dependent inhibition assay was performed.[45] As shown in Fig. 6, EGFR irreversible inhibitor PD168393 at 10 nM inhibited EGFR tyrosine kinase activity in a time-dependent manner; however, the inhibitory activity of reversible inhibitor Tarceva at 10 nM plateaued after incubation for 5 to 15 min. Under these conditions, compound **7d** inhibited EGFR tyrosine kinase activity in a concentration- and time-dependent manner (Fig. 6). These results suggest that the boron-conjugated 4-anilinoquinazoline **7d** irreversibly suppresses EGFR tyrosine kinase.

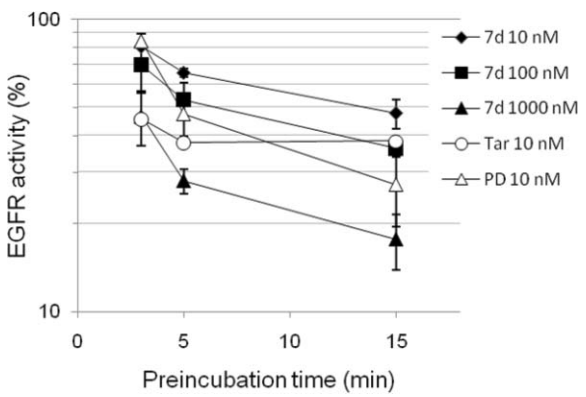

Fig. 6 Preincubation time-dependent inhibition of EGFR by compound **7d**. EGFR was incubated in kinase assay buffer with various concentrations of compound **7d**, 10 nM Tarceva (Tar), or 10 nM PD168393 (PD). After incubation for the indicated time, kinase assay was initiated by adding ATP (10 μM), and phosphorylation of the poly(Glu:Tyr) substrate was detected. The drug concentrations required to inhibit the phosphorylation of the poly(Glu:Tyr) substrate by 50% (IC_{50}) were determined from semilogarithmic dose–response plots, and results represent the mean ± s.d. of triplicate samples.

Recently, the X-ray cocrystal structure of EGFR and PD168393 was reported and a covalent bond has been observed between the acrylamide Michael acceptor on PD168393 and the targeted Cys797 in the complex (PDB code: 2JF5).[21] We tried to detect the Cys797-containing peptide fragment VQLITQLMPFGCLLDYVREHKD, which was generated by treated with trypsin digestion of EGFR kinase domain, by ESI-TOF and MALDI-TOF mass spectroscopies in order to clarify the covalent bond interaction of compound **7d** and EGFR. However, this peptide fragment was not ionized enough to be detected by the mass spectroscopy under our tested conditions. In fact, no report has been found for detection of this peptide fragment by mass spectroscopic analysis. Fry and coworkers reported that the covalent conjugation of Cys773 in the fragment EILDEAYVMASVDNPHVCR with PD168393 was detected by ESI mass spectroscopy.[14] However, Cys773 is located near the aniline ring of both inhibitors Tarceva and PD168393 in the reported cocrystal structures.[21,22] Therefore, the report for detection of the covalent conjugation of Cys773 and PD168393 has exhibited the possibility of alternative binding mode of PD168393 in EGFR kinase domain. Since mass-spectroscopic analysis was not been suitable for clarification of the covalent bonding interaction of Cys797 and compound **7d**, we next demonstrated molecular docking and quantum mechanical simulation to predict the plausible binding mode of compound **7d** in the EGFR kinase domain.

Molecular docking and quantum mechanical simulation

We performed a molecular docking simulation of compound **7d** with the ATP-binding site of EGFR kinase domain (PDB code 1M17). The initial structure of protein backbone was taken from the X-ray structure of EGFR kinase domain in complex with Tarceva.[22] A conformation search for three rotatable bonds of compound **7d** (Fig. 7A) was performed to examine the boron docking mode toward surrounding residues. As shown in Fig. 7B, 65 conformers were observed and classified into three clusters. The boronic acid of compound **7d** was located around Cys797 or Asp800 in the clusters 1 and 2, respectively, suggesting interactions of the boronic acid with such residues. Based on these two conformations, three docking models (models 1–3) were constructed for further calculations. The initial structure of model 1 was selected from the cluster 2, and those of model 2 and model 3 were selected from the cluster 1. The thiol group of Cys797 was in neutral form (–SH) for model 1 and model 2, and negatively charged form ($–S^-$) for model 3.

The docking structure of Tarceva (X-ray structure) and the three models of compound **7d** were further optimized by using the ONIOM-QM/MM simulation at the HF/6-31G(d):UFF level of theory. As shown in Fig. 8, the QM region includes both interaction sites of quinazoline ring and boronic acid moieties: binding site residues of EGFR, a hydrogen-bonding water molecule, and inhibitor. Fig. 9 shows the three docking modes

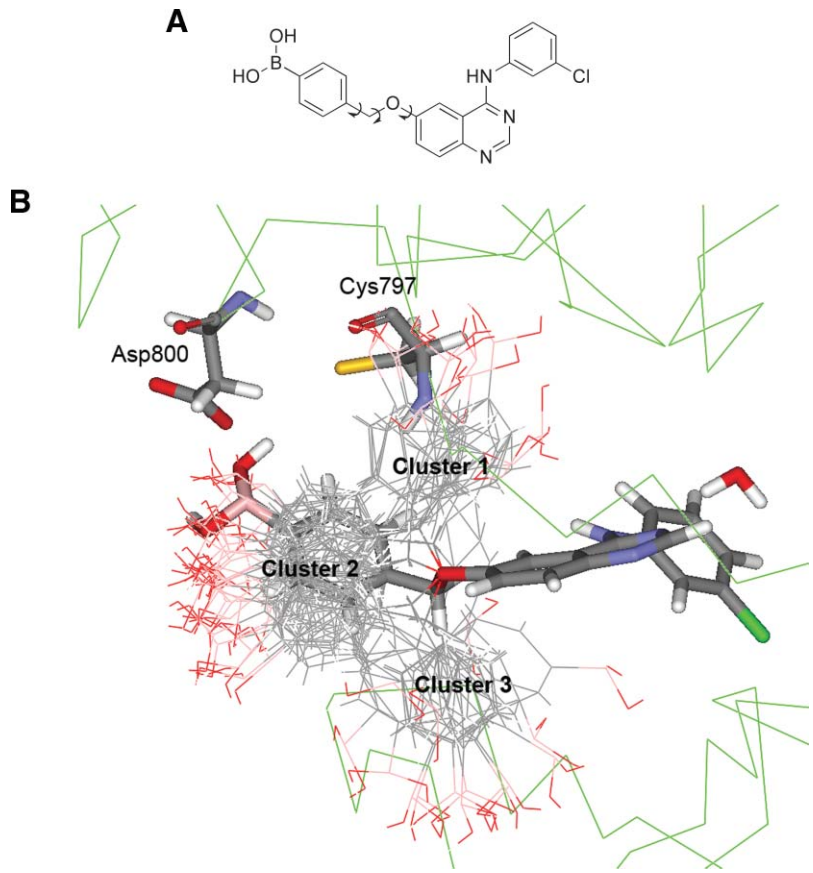

Fig. 7 Conformation search results of compound **7d**. (A) Rotatable bonds used for conformation search of compound **7d**. (B) The line representation refers to searched inhibitor structure: the stick representation refers to Cys797, Asp800, and initial geometry of inhibitor: the trace line representation is the Cα backbone.

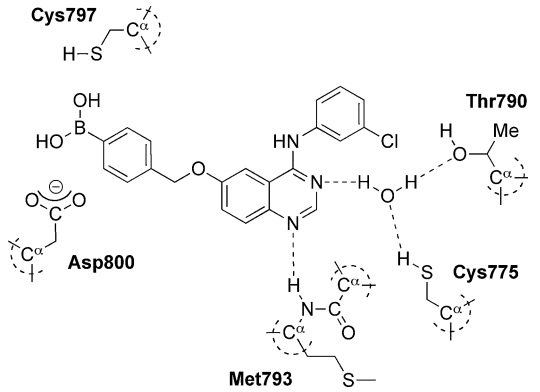

Fig. 8 High-level quantum mechanical (QM) region in the ONIOM calculation. Both side chains and backbones were capped at the Cα positions (dotted curves) by using hydrogen link atoms. Dotted lines indicate hydrogen bonds between the EGFR and inhibitor.

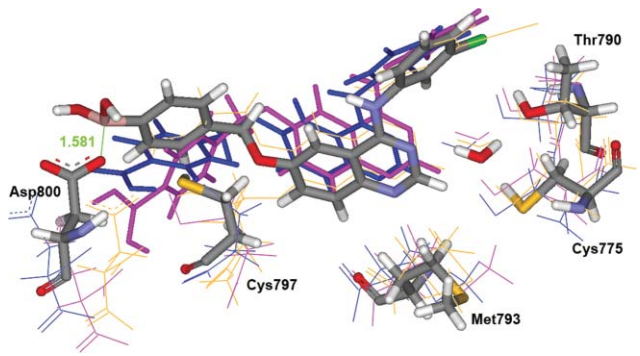

Fig. 9 Binding modes of compound **7d** (models 1–3) overlaid with the binding conformation of Tarceva into the active site of EGFR kinase domain. Model 1, model 2 and model 3 are shown with backbone colors of pink, blue, and yellow, respectively.

of the compound **7d** (models 1–3) into the active site of EGFR kinase domain overlaid with the binding conformation of Tarceva (schematic figures and geometrical values for each docking mode are available in the ESI†). According to the simulation, the 4-anilinoquinazoline moieties of both compound **7d** and Tarceva bind to the kinase domain in a similar manner. In all binding structures, three hydrogen bonds were observed as well as the X-ray structure: one direct hydrogen bond between the nitrogen (N1) of the quinazoline ring and the amide nitrogen of Met793 (N–H lengths 2.28–2.44 Å); two hydrogen bonds mediated by single water molecule among the nitrogen (N3) of the quinazoline ring, the thiol hydrogen of Cys775, and hydroxyl oxygen of Thr790. The corresponding calculated values are 2.28–2.40 Å between N3 and the water hydrogen; 2.32–2.65 Å between the thiol hydrogen of Cys775 and the water oxygen; 2.02–2.05 Å between the hydroxyl oxygen of Thr790 and the water hydrogen. Also, the chloro group on the aniline ring of compound **7d** is located in a very similar position to the ethynyl group of Tarceva. In the binding structures of compound **7d** (models 1–3), additional bonds were observed at the boronic acid site. Model 1 indicated a covalent B–O bond between the sp^3-hybridized boron atom and the carboxyl oxygen atom of Asp800. The calculated B–O distance is 1.58 Å, which is longer than other two B–O lengths in the boronic acid (1.44 and 1.42 Å). In contrast, the hybridization state of boron atom was

Table 2 Calculated binding energies (in kcal/mol) between EGFR and inhibitors

Compound	Boron hybridization	ΔE
7d – model 1	sp^3	–90.2190
7d – model 2	sp^2	–50.9435
7d – model 3	sp^2	–56.3295
Tarceva	—	–33.6273

sp^2 for models 2 and 3. A strong hydrogen bond between hydroxyl hydrogen of boronic acid and carboxyl oxygen atom of Asp800 was observed, with lengths of 1.60 and 1.73 Å for models 2 and 3, respectively. A second hydrogen bond was also observed in model 3 between the other hydroxyl hydrogen of boronic acid and thiol ion S^- of Cys797, with a length of 2.43 Å. Therefore, the interaction between the EGFR and inhibitor at the boronic acid site is even stronger than that of the quinazoline ring site, and this covalent interaction may induce the prolonged inhibition of compound **7d** toward EGFR tyrosine kinase.

For a quantitative evaluation of the EGFR–inhibitor interaction, binding energies of each binding mode were calculated based on the *ab initio* FMO method. The energy of each of the three systems, *i.e.*, the receptor (E_{EGFR}), the inhibitor ($E_{linhibitor}$), and their complex ($E_{complex}$) were calculated, where the hydrogen-bonded water molecule was included in the receptor. The binding energy, ΔE, can be obtained by the following equation:

$$\Delta E = E_{complex} - (E_{EGFR} + E_{linhibitor}) \quad (1)$$

The calculated ΔE values are summarized in Table 2. For all binding models of compound **7d**, absolute values of ΔE were larger than that of Tarceva due to additional covalent and hydrogen bonds at the boronic acid site. The strongest interaction between the EGFR and **7d** was observed for model 1 with a ΔE value of –90.2 kcal/mol. The existence of a B–O covalent bond between boronic acid and Asp800 supports such a strong interaction. Model 2 and model 3 indicate a medium degree of interactions, –50.9 and –56.3 kcal/mol, respectively, hydrogen bonds between the boronic acid and Cys797 and Aps800 causing the stabilization. Therefore, model 1 is energetically preferred as the binding form of compound **7d** toward EGFR tyrosine kinase.

Conclusions

In the present study, we designed boron-conjugated 4-anilinoquinazolines as inhibitors of EGFR tyrosine kinase with possible covalent bond interactions between the boron atom and the nucleophilic thiol of the EGFR kinase domain. Selective inhibition of boron-conjugated 4-anilinoquinazolines was observed at 1 μM; compound **6c** exhibited significant inhibition of EGFR tyrosine kinase with an IC_{50} value of 0.19 μM. Boron compounds also reduced the proliferation of A431 cells, selectively, with GI_{50} values of 0.53–2.42 μM. Among the compounds synthesized, compounds **6c**, **7b**, and **7d** significantly suppressed the EGF-induced phosphorylation of ERK and Akt in parallel with the inhibition of EGFR autophosphorylation in A431 cells, and compound **7d** was found to possess prolonged inhibitory activity toward autophosphorylation of EGFR tyrosine kinase at 5 h after cell wash, although inhibition of the cell growth was not

particularly high in comparison with other compounds. Flow cytometry analysis of compounds **6c**, **7b**, and **7d** revealed that these compounds induced G1 arrest in cell cycle and apoptosis. Docking studies suggest that the quinazoline ring of compound **7d** is bound to the EGFR kinase domain in a very similar manner to that of Tarceva. The boronic acid moiety of compound **7d** is shown to be able to form a covalent B–O bond with Asp800 and hydrogen bonds with Cys797 and Asp800, which may cause the prolonged inhibition of EGFR tyrosine kinase by compound **7d**. Although the acidity of each boronic acid and physico-chemical nature of aromatic and aliphatic boronic acids should affect the binding to the protein, these results suggest that boron has potential in pharmaceutical drug design for prolonged interaction to target proteins through covalent bonds.

Experimental

General methods

^{1}H NMR and ^{13}C NMR spectra were measured on JEOL JNM-AL 300 (300 MHz) and VARIAN UNITY-INOVA 400 (400 MHz) spectrometers. Chemical shifts of ^{1}H NMR and ^{13}C NMR are expressed in parts per million (ppm, δ units), and coupling constants are expressed in units of hertz (Hz). IR spectra were measured on a Shimadzu FTIR-8200A spectrometer. Analytical thin-layer chromatography (TLC) was performed on glass plates (Merck Kieselgel 60 F_{254} or RP-18 F_{254}, layer thickness 0.2 mm). Samples were visualized by UV light (254 nm), I_2, or $KMnO_4$. Column chromatography was performed on silica gel (Merck Kieselgel 70–230 mesh). All reactions were carried out under argon atmosphere using standard Schlenk techniques. Most chemicals were of analytical grade and used without further purification.

6-Hydroxy-4(1*H*)-quinazolinone (2)

To a solution of hydroxyanthranilic acid **1** (12.7 g, 83 mmol) in THF (300 ml) was added ethyl chloroformate (23.8 ml, 249 mmol) and the reaction mixture was refluxed for 24 h. The solvent was removed under reduced pressure. The resulting residue was dissolved in diethyl ether (300 ml) and PBr_3 (15.3 ml, 84 mmol) was added. The mixture was stirred at 50 °C for 24 h and cooled to room temperature. After addition of water (200 ml), the white precipitate was filtered and dried *in vacuo*. The resulting solid was dissolved in formamide (198 ml, 5.0 mol) and the reaction mixture was refluxed for 24 h. After the mixture was cooled to room temperature, water (100 ml) was added. The precipitate was filtered and washed with water (100 ml) to give **2** (9.45 g, 70%) as a yellow solid: ^{1}H NMR (300 MHz, CD_3OD) δ = 7.87 (s, 1H), 7.48 (d, J = 6.0 Hz, 1H), 7.41 (d, J = 3.0 Hz, 1H), 7.21 (dd, J = 6.0, 3.0 Hz, 1H);^{13}C NMR (75 MHz, CD_3OD) δ = 163.5, 158.7, 143.7, 134.7, 129.7, 125.8, 125.1, 110.4; IR (KBr) 3078, 1670, 1653, 1508, 1489, 1340, 1248 cm^{-1}; HRMS(ESI) calcd for $C_8H_7N_2O_2$ [M + H]$^+$: m/z 163.0508, found m/z 163.0503.

3,4-Dihydro-4-oxoquinazolin-6-yl acetate (3)

To a solution of **2** (1.0 g, 6.5 mmol) and triethylamine (0.2 ml, 1.3 mmol) in dichloromethane (40 ml) were added acetic anhydride (1.8 ml, 19 mmol) and dimethylaminopyridine (24 mg, 0.2 mmol) at 0 °C and the reaction was allowed to warm at room temperature for 1 h. The solvent was removed under reduced pressure and the residue was purified by silica gel column chromatography with dichloromethane/methanol (20:1) to give **3** (1.26 g, 95%) as a yellow solid: ^{1}H NMR (400 MHz, $CDCl_3$) δ = 10.95 (bs, 1 H), 8.97 (s, 1 H), 8.01 (d, J = 2.8 Hz, 1 H), 7.80 (d, J = 8.8 Hz, 1 H), 7.54 (dd, J = 8.8 Hz, 2.8 Hz, 1 H), 2.36 (s, 3 H); ^{13}C NMR (75 MHz, $CDCl_3$) δ = 169.0, 149.4, 146.7, 142.9, 129.3, 129.1, 123.4, 118.4, 20.9; IR (KBr) 3067, 2910, 1684, 1653, 1434, 1229, 835 cm^{-1}; MS(ESI) m/z 227 [M+Na]$^+$.

4-Chloroquinazolin-6-yl acetate (4)

To a solution of **3** (1.15 g, 5.64 mmol) in dichloromethane (40 ml) were added $POCl_3$ (0.64 ml, 6.8 mmol) and ethyl diisopropylamine (1.27 ml, 14 mmol) and the mixture was refluxed for 12 h. The solvent was removed under reduced pressure and the residue was purified by silica gel column chromatography with hexane/ethyl acetate (1/1) to give **4** (1.0 g, 80%) as a yellow solid:^{1}H NMR (400 MHz, $CDCl_3$) δ = 9.05 (s, 1 H), 8.11 (d, J = 8.8 Hz, 1 H), 8.01 (d, J = 2.4 Hz, 1 H), 7.73 (dd, J = 8.8, 2.4 Hz, 1 H), 2.40 (s, 3 H); ^{13}C NMR (75 MHz, $CDCl_3$) δ = 168.9, 162.0, 153.5, 150.1 149.1, 130.5, 124.5, 116.8, 21.0; IR (KBr) 1869, 1757, 1684, 1653, 1558, 1508, 1205, 1177 cm^{-1}; MS(ESI) m/z 245 [M+Na]$^+$.

4-(3-Chloroanilino)-6-hydroxyquinazoline (5)

To a solution of **4** (839 mg, 3.8 mmol) in isopropanol (5 ml) was added 3-chloroaniline (1.0 ml, 9.4 mmol) and the mixture was refluxed for 12 h. The solvent was removed under reduced pressure and the residue was dissolved in methanol (20 ml). The 25% aqueous ammonia solution (4 ml) was added and the mixture was stirred at room temperature for 12 h. The solvent was removed until the solid was precipitated and the resulting solid was filtered, washed with dichloromethane (20 ml), and dried *in vacuo* to give **5** (1.0 g, >99%) as a pale yellow solid:^{1}H NMR (400 MHz, CD_3OD) δ = 8.35 (s, 1 H), 7.88 (t, J = 1.6 Hz, 1 H), 7.59 (d, J = 9.2 Hz, 1 H), 7.55 (d, J = 2.4 Hz, 1 H), 7.33 (dd, J = 2.4 Hz, 9.2 Hz, 1 H), 7.26 (t, J = 8.0 Hz, 1 H), 7.05 (dt, J = 2.0, 8.0 Hz, 1 H);^{13}C NMR (75 MHz, CD_3OD_3) δ = 159.2, 158.1, 152.9, 145.0, 136.3, 135.5, 131.2, 129.8, 126.0, 125.4, 123.8, 122.1, 118.2, 106.0; IR (KBr) 2654, 1622, 1595, 1570, 1541, 1447, 1396 cm^{-1}; MS(ESI) m/z 272 [M + H]$^+$; Analysis calculated for $C_{17}H_{10}ClN_3O$: C, 61.89; H, 3.71; N, 15.47. Found: C, 58.25; H, 3.55; N, 15.57.

Synthesis of boronic esters (8–13)

2-(3-Chloropropenyl)-4,4,5,5-tetramethyl-[1,3,2]dioxaborolane (8). A mixture of *trans*-3-chloro-1-propenylboronic acid (120 mg, 1.0 mmol) and pinacol (118 mg, 1.0 mmol) in Et_2O (5 ml) was stirred at room temperature for 24 h. The mixture was dried over $MgSO_4$ and concentrated to give **8** (202 mg, 99%) as a yellow oil: ^{1}H NMR (300 MHz, $CDCl_3$) δ = 6.64 (dt, J = 18.0, 6.0 Hz, 1H), 5.74 (dt, J = 18.0, 3.0 Hz, 1H), 4.10 (dd, J = 6.0, 3.0 Hz, 2H), 1.25 (s, 12H); ^{13}C NMR (75 MHz, $CDCl_3$) δ = 146.6, 83.5, 83.2, 46.0, 24.7; IR (neat) 3404, 2980, 2934, 1643, 1475, 1358, 1146,851 cm^{-1}; MS(ESI) m/z 203 [M + H]$^+$; Analysis calculated for $C_9H_{16}BClO_2$: C, 53.38; H, 7.96. Found: C, 53.34; H, 7.90.

4-(3-Chloropropenyl)-2,9,9-trimethyl-3,5-dioxa-4-boratricyclo-[6.1.1.0^{2},6]decane (9). Synthesized from *trans*-3-chloro-1-propenylboronic acid (602 mg, 5.0 mmol) and (1S, 2S, 3R, 5S)-(+)-pinandiol (851 mg, 5.0 mmol) using the procedure described for **8** to give **9** (624 mg, 49%) as a yellow oil:^{1}H NMR (400 MHz, $CDCl_3$) $\delta = 6.64$ (dt, $J = 18.0$, 6.0 Hz, 1 H), 5.77 (dt, $J = 18.0$, 10.2 Hz, 1 H), 4.32 (dd, $J = 8.8$, 1.6 Hz, 1 H), 4.11 (dd, $J = 6.0$, 1.2 Hz, 2 H), 2.35 (ddt, $J = 14.4$, 8.8, 2.0 Hz, 1 H), 2.22 (m, 1 H), 2.07 (t, $J = 6.0$ Hz, 1 H), 1.85–1.94 (m, 2 H), 1.41 (s, 3 H), 1.19 (d, $J = 10.4$ Hz, 1 H), 1.29 (s, 3 H), 0.85 (s, 3 H); ^{13}C NMR (75 MHz, $CDCl_3$) $\delta = 146.5$, 101.3, 85.9, 77.9, 51.2, 46.0, 39.4, 38.1, 35.3, 28.5, 27.0, 26.4, 23.9; IR (neat) 2920, 2872, 1643, 1362, 1283, 1030, 851 cm^{-1}; Analysis calculated for $C_{13}H_{20}BClO_2$: C, 61.34; H, 7.92. Found: C, 61.44; H, 7.88.

4-Bromomethyl-2,9,9-trimethyl-3,5-dioxa-4-bora-tricyclo-[6.1.1.0^{2,6}]decane ($(RO)_2BCH_2Br$, 10). To a solution of dibromoethane (4.2 ml, 6.0 mmol) and triisopropylborate (6.0 mmol) in THF (30 ml) was added *n*-BuLi (1.6 M in hexanes, 1.4 ml, 6.0 mmol) at −80 °C with stirring. After 30 min, methanesulfonic acid (0.4 ml, 6.0 mmol) was added at −80 °C and then the reaction mixture was stirred at room temperature for 24 h. Solvent was removed under reduced pressure and the residue was purified by silica gel column chromatography with hexane/ethyl acetate (10/1) to give **10** (1.5 g, 92%) as a colorless oil: ^{1}H NMR (400 MHz, $CDCl_3$) $\delta = 4.38$ (dd, $J = 8.8$, 1.6 Hz, 1 H), 2.64 (s, 2 H), 2.36 (m, 1 H), 2.26 (m, 1 H), 2.08 (t, $J = 8.4$ Hz, 1 H), 1.87–1.98 (m, 2 H), 1.48 (m, 3 H), 1.31 (m, 3 H), 1.19 (d, $J = 10.8$ Hz, 1 H), 0.89 (s, 3 H); ^{13}C NMR (75 MHz, $CDCl_3$) $\delta = 86.8$, 78.6, 51.2, 39.3, 38.2, 35.2, 28.3, 26.9, 26.3, 23.9; IR (neat) 2922, 2872, 1416, 1384, 1339, 1286, 1030, 845 cm^{-1}; Analysis calculated for $C_{11}H_{18}BBrO_2$: C, 48.40; H 6.65. Found: C, 48.28; H, 6.70.

4-(2,9,9-Trimethyl-3,5-dioxa-4-boratricyclo[6.1.1.0^{2},6]dec-4-yl)-benzaldehyde (11). Synthesized from 4-formylphenylboronic acid (750 mg, 5.0 mmol) and (1*S*,2*S*,3*R*,5*S*)-(+)-pinandiol (851 mg, 5.0 mmol) using the procedure described for **8** to give **11** (1.42 g, 99%) as a white solid: ^{1}H NMR (400 MHz, $CDCl_3$) $\delta =$ 10.06 (s, 1 H), 7.98 (d, $J = 9.0$ Hz, 2 H), 7.87 (d, $J = 9.0$ Hz, 2 H), 4.48 (d, $J = 9.0$ Hz, 1 H), 2.43 (m, 1 H), 2.23 (m, 1 H), 2.17 (t, $J =$ 6.0 Hz, 1 H), 1.95–2.02 (m, 2 H), 1.51 (s, 3 H), 1.32 (s, 3 H), 1.19 (d, $J = 12.0$ Hz, 1 H), 0.90 (s, 3 H); ^{13}C NMR (75 MHz, $CDCl_3$) $\delta = 192.6$, 138.0, 135.2, 128.7, 86.7, 78.5, 51.3, 39.4, 38.2, 35.4, 28.6, 27.0, 26.4, 24.0; IR (KBr) 2976, 2916, 2731, 1705, 1508, 1350, 1205, 1088, 827 cm^{-1}. Analysis calculated for $C_{17}H_{21}BO_3$: C, 71.86; H, 7.45. Found: C, 72.15; H, 7.60.

[4-(2,9,9-Trimethyl-3,5-dioxa-4-boratricyclo[6.1.1.0^{2,6}]dec-4-yl)-phenyl]methanol (12). To a solution of **11** (1.42 g, 5.0 mmol) in methanol (30 ml) was added $NaBH_4$ (473 mg, 12 mmol) at −40 °C and the reaction mixture was stirred at room temperature for 1 h. The solvent was removed under reduced pressure, and the residue was dissolved in water (30 ml) and extracted with dichloromethane (2 × 50 ml). The combined organic layer was dried over $MgSO_4$ and concentrated. Purification by silica gel column chromatography with hexane/ethyl acetate (1/1) gave **12** (1.0 g, 71%) as a colorless oil: ^{1}H NMR (400 MHz, $CDCl_3$) $\delta =$ 7.81 (d, $J = 8.0$ Hz, 2 H), 7.38 (d, $J = 8.0$ Hz, 2 H), 4.72 (d, $J = 6.0$ Hz, 2 H), 4.45 (dd, $J =$2.0, 8.8 Hz, 1 H), 2.41 (m, 1 H), 2.26 (m, 1 H), 2.15 (t, $J = 6.0$ Hz, 1 H), 1.84–2.06 (m, 2 H), 1,48 (s, 3 H), 1,31 (s, 3 H), 1,21 (d, $J = 10.8$ Hz, 1 H), 0.89 (s, 3 H); ^{13}C NMR (75 MHz, $CDCl_3$) $\delta = 135.1$, 126.1, 125.8, 101.3, 86.2, 78.2, 65.3, 51.4, 39.5, 38.1, 35.5, 28.6, 27.0, 26.4, 24.0; IR (neat) 3433, 2920, 2870, 1614, 1402, 1362, 1236, 1092, 1020, 820 cm^{-1}; Analysis calculated for $C_{17}H_{23}BO_3$: C, 71.35; H, 8.10. Found: C, 71.41; H, 8.15.

4-(4-Bromomethylphenyl)-2,9,9-trimethyl-3,5-dioxa-4-boratricyclo[6.1.1.0^{2,6}]decane (13). To a solution of 12 (1.0 g, 3.5 mmol) in toluene (20 ml) was added phosphorus tribromide (0.34 ml, 3.5 mmol) at 0 °C and the reaction was allowed to warm at room temperature. After 3 h, water (30 ml) was added and the reaction mixture was then extracted with dichloromethane (2 × 50 ml). The combined organic layer was dried over $MgSO_4$ and concentrated. Purification by silica gel column chromatography with hexane/ethyl acetate (1/1) gave **13** (658 mg, 53%) as a green oil: ^{1}H NMR (300 MHz, $CDCl_3$) $\delta = 7.79$ (d, $J = 9.0$ Hz, 2 H), 7.40 (d, $J = 9.0$ Hz, 2 H), 4.50 (s, 2 H), 4.45 (d, $J = 9.0$ Hz, 1 H), 2.42 (m, 1 H), 2.25 (m, 1 H), 2.15 (t, $J = 6.0$ Hz, 1 H), 1.90–2,04 (m, 2 H), 1.48 (s, 3 H), 1.31 (s, 3 H), 1.20 (d, $J = 9.0$ Hz, 1 H), 0.89 (s, 3 H); ^{13}C NMR (75 MHz, $CDCl_3$) $\delta = 140.6$, 135.3, 128.3, 86.3, 78.3, 51.3, 39.5, 38.1, 35.5, 33.3, 28.6, 27.0, 26.4, 24.0; IR (neat) 2920, 2870, 1614, 1402, 1362, 1236, 1091, 1022 cm^{-1}; MS(ESI) *m/z* 373 [M+Na]$^{+}$; Analysis calculated for $C_{17}H_{22}BBrO_2$: C, 58.49; H 6.35. Found: C, 58.25; H, 6.62.

4-(3-Chloroanilino)-6-[3-(4,4,5,5-tetramethyl-[1,3,2]dioxaborolan-2-yl)-allyloxy]quinazoline (6a)

To a solution of sodium hydride (60% in oil, 32 mg, 0.8 mmol) in *N*,*N*′-dimethylformamide (DMF, 2 ml) was added **5** (107 mg, 0.4 mmol) at 0 °C and the reaction was allowed to warm at room temperature. After 30 min, the solution of boronic ester **8** (81 mg, 0.4 mmol) in DMF (3 ml) was added and the mixture was stirred for 2 h. Water (10 ml) was added and the reaction mixture was extracted with diethyl ether (50 ml). The solvent was removed under reduced pressure and the residue was purified by silica gel column chromatography with hexane/ethyl acetate (1/1) to yield **6a** (12mg, 7%) as a yellow solid:^{1}H NMR (300 MHz, $CDCl_3$): $\delta =$ 8.72 (s, 1 H), 7.92 (s, 1 H), 7.85, (d, $J = 9.0$ Hz, 1 H), 7.60 (d, $J = 9.0$ Hz, 1 H), 7.84 (dd, $J = 3.0$, 9.0 Hz, 1 H), 7.60 (d, $J =$ 9.0 Hz, 1 H), 7.48 (dd, $J = 9.0$, 3.0 Hz, 1 H), 7.33 (t, $J = 9.0$ Hz, 1 H), 7.14 (d, $J = 9.0$ Hz, 1 H), 7.10 (s, 1 H), 6.79 (dt, $J = 18.0$, 3.0 Hz, 1 H), 5.88 (d, $J = 18.0$ Hz, 1 H), 4.77 (d, $J = 3.0$ Hz, 2 H), 1.27 (s, 12 H); ^{13}C NMR (75 MHz, $CDCl_3$): $\delta = 157.0$, 156.4, 152.7, 145.9, 139.6, 134.7, 130.7, 130.0, 124.6, 124.3, 121.6, 119.5, 115.5, 101.0, 83.6, 77.2, 69.9, 24.8; IR (KBr) 2980, 2932, 1599, 1576, 1525, 1506, 1431, 1373, 1225, 1142, 839cm^{-1}; MS(ESI) *m/z* 438 [M + H]$^{+}$; Analysis calculated for $C_{23}H_{25}BClN_3O_3$: C, 63.11; H, 5.76; N, 9.60. Found: C, 63.40; H, 5.96; N 9.32.

4-(3-Chloroanilino)-6-[3-(2,9,9-trimethyl-3,5-dioxa-4-boratricyclo[6.1.1.0^{2},6]dec-4-yl)-allyloxy]quinazoline (6b)

Synthesized from **5** (381 mg, 1.5 mmol), **9** (407 mg, 1.5 mmol) using the procedure described for **6a**, to give **6b** (145 mg, 19%) as a yellow solid: ^{1}H NMR (400 MHz, $CDCl_3$) $\delta = 8.71$ (s, 1H), 7.78–7.87 (m, 3 H), 7.58 (d, $J = 8.0$ Hz, 1 H), 7.46 (dd, $J = 9.2$,

2.4 Hz, 1 H), 7.29 (t, $J = 8.0$ Hz, 1 H), 7.21 (d, $J = 2.4$ Hz, 1 H), 7.10 (dt, $J = 8.0$, 0.8 Hz, 1 H), 6.74 (dt, $J = 18.0$, 4.4 Hz, 1 H), 5.84 (d, J =18.0 Hz, 1 H), 4.65 (d, $J = 4.4$ Hz, 2 H), 4.32 (d, $J =$ 8.4 Hz, 1 H), 2.35 (m, 1 H), 2.20 (m, 1 H), 2.16 (t, $J = 8.4$ Hz, 1 H), 1.90 (m, 2 H), 1.41 (s, 3 H), 1.28 (s, 3 H), 1.12 (d, $J = 11.2$ Hz, 1 H), 0.84 (s, 3 H); ^{13}C NMR (75 MHz, $CDCl_3$) $\delta = 157.0$, 156.6, 152.7, 145.9, 139.7, 134.6, 130.5, 129.9, 124.5, 124.2, 121.7, 119.6, 115.6, 101.4, 85.9, 77.9, 69.9, 51.3, 39.5, 38.1, 35.4, 28.6, 27.1, 26.4, 23.9; IR (KBr) 2918, 2870, 1526, 1429, 1410, 1369, 1227, 839 cm^{-1}; MS(ESI) m/z 490 [M+MeOH]$^+$; Analysis calculated for $C_{27}H_{29}BClN_3O_3$: C, 66.21; H, 5.97; N 8.58. Found: C, 66.11; H, 6.12; N, 8.53.

4-(3-Chloroanilino)-6-(2,9,9-trimethyl-3,5-dioxa-4-boratricyclo[6.1.1.0^2,6]dec-4-ylmethoxy)quinazoline (6c)

Synthesized from **5** (271 mg, 1.0 mmol) and **10** (286 mg, 1.0 mmol) using the procedure described for **6a**, to give **6c** (91 mg, 19%) as a yellow solid: ^{1}H NMR (400 MHz, $CDCl_3$) $\delta = 8.73$ (s, 1 H), 7.95 (t, $J = 2.0$ Hz, 1 H), 7.86 (d, $J = 8.8$ Hz, 1 H), 7.59 (dd, $J = 9.2$, 1.2 Hz, 1 H), 7.55 (dd, $J = 9.2$, 2.4 Hz, 1 H), 7.41 (bs, 1 H), 7.32 (t, $J = 8.0$ Hz, 1 H), 7.21 (d, $J = 2.4$ Hz, 1 H), 7.12 (dt, $J = 8.0$, 1.2 Hz, 1 H), 4.42 (d, $J = 8.0$ Hz, 1 H), 4.01 (s, 2 H), 2.38 (m, 1 H), 2.24 (m, 1 H), 2.12 (t, $J = 8.4$ Hz, 1 H), 1.92 (m, 2 H), 1.46 (s, 3 H), 1.30 (s, 1 H), 1.19 (d, $J = 12.0$ Hz, 1 H), 0.86 (s, 3 H);^{13}C NMR (75 MHz, $CDCl_3$) $\delta = 158.8$, 156.4, 152.6, 145.6, 139.8, 134.7, 130.5, 129.9, 124.1, 124.0, 121.3, 119.2, 115.5, 100.4, 87.1, 78.6, 51.2, 39.5, 38.2, 35.2, 28.6, 27.0, 26.6, 23.9; IR (KBr) 2926, 2870, 1579, 1560, 1521, 1435, 1209, 1128, 1015, 841 cm^{-1}; MS(ESI) m/z 486 [M+Na]$^+$; Analysis calculated for $C_{25}H_{27}BClN_3O_3$: C, 64.75; H, 5.87; N, 9.06. Found: C, 64.88; H, 5.80; N, 9.13.

4-(3-Chloroanilino)-6-[4-(2,9,9-trimethyl-3,5-dioxa-4-boratricyclo[6.1.1.0^2,6]dec-4-yl)-benzyloxy]quinazoline (6d)

Synthesized from **5** (271 mg, 1.0 mmol) and **13** (349 mg, 1.0 mmol) using the procedure described for **6a**, to give **6d** (297 mg, 52%) as a yellow solid:^{1}H NMR (400 MHz, $CDCl_3$) $\delta = 8.73$ (s, 1 H), 7.93 (t, $J = 2.0$ Hz, 1 H), 7.87–7.90 (m, 1 H), 7.75–7.83 (m, 1 H), 7.55 (m, 2 H), 7.49 (d, $J = 8.0$ Hz, 2 H), 7.34 (t, $J = 8.0$ Hz, 1 H), 7.15 (s, 1 H), 7.14 (d, $J = 8.0$ Hz, 1 H), 5.25 (s, 2 H), 4.47 (d, $J =$ 7.2 Hz, 1 H), 2.44 (m, 1 H), 2.24 (m, 1 H), 2.16 (t, $J = 5.2$ Hz, 1 H), 1.92 (m, 2 H), 1.50 (s, 3 H), 1.32 (s, 3 H), 1.20 (d, $J = 10.8$ Hz, 1 H), 0.89 (s, 3 H);^{13}C NMR (75 MHz, $CDCl_3$) $\delta = 157.1$, 156.4, 152.8, 145.7, 139.6, 139.0, 135.3, 134.7, 130.7, 129.9, 126.6, 124.5, 124.2, 121.5, 119.4, 115.5, 101.3, 86.4, 78.3, 51.4, 39.5, 38.2, 35.5, 28.6, 27.0, 26.4, 24.0; IR (KBr)2918, 2870, 1570, 1528, 1404, 1364, 1229, 1092, 1020, 837 cm^{-1}; MS(ESI) m/z 540 [M + H]$^+$; Analysis calculated for $C_{31}H_{31}BClN_3O_3$: C, 68.97; H, 5.79; N, 7.78. Found: C, 68.91; H, 5.59; N, 7.78.

4-[4-(3-Chloroanilino)quinazolin-6-yloxy]but-2-enylboronic acid (7b)

To a solution of **6b** (142 mg, 0.29 mmol) in methanol (10 ml) was added KHF_2 (158 mg, 2.0 mmol) in water (10 ml), and the reaction mixture was stirred at room temperature for 2 h. The solvent was removed and the residue was dissolved in acetonitrile (5 ml) and hexane (9 ml). Phenyl boronic acid (73 mg, 0.6 mmol) was added and then the mixture was stirred at room temperature for 1 h. The acetonitrile phase was separated and concentrated. The residue was purified by silica gel column chromatography with dichloromethane/ethanol (30/1) to give **7b** (18.9 mg, 18%) as a yellow solid: ^{1}H NMR (400 MHz, CD_3OD) $\delta = 8.37$ (s, 1 H), 7.86 (t, J =2.0Hz, 1 H), 7.66 (d, $J = 2.4$ Hz, 1 H), 7.57–7.63 (m, 2 H), 7.43 (dd, $J = 9.2$, 2.4 Hz, 1 H), 7.25 (t, $J =$ 8.0 Hz, 1 H), 7.23 (bs, 1 H), 7.04 (d, $J = 9.2$ Hz, 1 H), 6.61 (dt, $J = 16.0$, 4.4 Hz, 1 H), 5.91 (d, J =16.0 Hz, 1 H), 4.69 (d, $J =$ 4.4 Hz, 2 H);^{13}C NMR (75 MHz, CD_3OD) $\delta = 159.3$, 159.0, 153.5, 146.2, 142.0, 135.5, 131.2, 129.9, 126.5, 125.5, 123.9, 122.1, 117.6, 104.3, 71.5; IR (KBr) 2926, 2855, 1597, 1560, 1526, 1508, 1364, 1227, 1063, 995, 835 cm^{-1}; Analysis calculated for $C_{17}H_{15}BClN_3O_3$: C, 57.42; H, 4.25; N, 11.82. Found: C, 57.45; H, 4.35; N 11.76.

[4-(3-Chloroanilino)quinazolin-6-yloxy]methylboronic acid (7c)

Synthesized from **6c** (136 mg, 0.24 mmol) and KHF_2 (137 mg, 1.75 mmol) using the procedure described for **7b**, to give **7c** (19.8 mg, 19%) as a yellow solid:^{1}H NMR (400 MHz, CD_3OD) δ=8.48 (s, 1 H), 7.88 (bs, 1 H), 7.72 (bs, 1 H), 7.53–7.62 (m, 2 H), 7.47 (d, $J = 9.2$ Hz, 1 H), 7.27 (t, $J = 8.0$ Hz, 1 H), 7.07 (d, $J = 8.0$ Hz, 1 H), 3.35 (s, 2 H);^{13}C NMR (75 MHz, CD_3OD) $\delta = 159.1$, 155.6, 152.3, 146.5, 142.5, 135.3, 131.0, 129.4, 125.1, 125.0, 124.4, 122.0, 120.3, 118.8, 55.6; IR (KBr) 2924, 2852, 1558, 1541, 1522, 1508, 1387, 1340, 1225 cm^{-1}; Analysis calculated for $C_{15}H_{13}BClN_3O_3$: C, 54.67; H, 3.98; N, 12.75. Found: C, 54.55; H, 3.70; N, 12.91.

4-[4-(3-Chloroanilino)quinazolin-6-yloxymethyl]phenylboronic acid (7d)

Synthesized from **6d** (15 mg, 32 μmol) and KHF_2 17.5 mg, 0.22 mmol) using the procedure described for **7b**, to give **7d** (3.0 mg, 28%) as a yellow solid:^{1}H NMR (400 MHz, CD_3OD) $\delta = 8.43$ (s, 1 H), 7.85 (dd, $J = 7.2$, 2.4 Hz, 2 H), 7.50–7.67 (m, 5 H), 7.39 (m, 2 H), 7.27 (t, $J = 8.0$ Hz, 1 H), 7.07 (d, $J = 8.0$ Hz, 1 H), 5.16 (s, 2 H);^{13}C NMR (75 MHz, CD_3OD) δ =159.6, 159.5, 153.0, 144.2, 141.6, 135.5, 153.2, 131.3, 128.7, 128.1, 127.4, 127.1, 125.9, 124.1, 122.4, 117.4, 104.7, 72.0; IR (KBr) 2903, 2856, 1579, 1570, 1528, 1508, 1380, 1251, 1016, 833cm^{-1}; Analysis calculated for $C_{21}H_{17}BClN_3O_3$: C, 62.18; H, 4.22; N, 10.36. Found: C, 62.46; H, 4.38; N, 10.40.

Kinase assays

The kinase activity of various tyrosine kinases was determined by ELISA.[38] EIA/RIA Stripwell™ plates (Corning) were coated by incubation overnight at 4 °C with 100 μl/well of 50 μg/ml poly(Glu:Tyr, 4:1) peptide (Sigma) in PBS. The kinase reaction was performed in the plates by addition of 50 μl of kinase buffer (50 mM HEPES, 125 mM NaCl, 10 mM $MgCl_2$, pH 7.4) containing ATP (10 μM), 10 ng of recombinant EGFR, HER2, Flt-1 or KDR (Invitrogen, catalytic domain), and inhibitors. After 20 min, the plates were washed three times with wash buffer (0.1% Tween 20 in PBS) and incubated for 20 min with 50 μl/well of 0.2 μg/ml HRP conjugated anti-phosphotyrosine antibody (Santa Cruz). After two washes, the plates were developed by addition of 50 μl/well tetramethylbenzidine (Sigma) and stopped by addition of 50 μl/well of 2 N H_2SO_4. The absorbance at 450 nm

was measured by a 96-well plate reader (Tecan). Preincubation-time dependent inhibition assay was generated based on previous methods.[45] The recombinant EGFR (10 ng) was incubated in kinase assay buffer containing various concentrations of drug except ATP. After incubation for 3, 5, or 15 min, the reaction was initiated by addition of ATP (10 μM) into the reaction mixture. Other procedures were performed as described above.

Cell growth assays

The human carcinoma cell lines, A431 (epidermoid carcinoma), HepG2 (liver carcinoma), KatoIII (gastric carcinoma), and SKBR3 (breast carcinoma) were used for the cell growth assay. Each cell line (5×10^3 cells/well of 96-well plate) was incubated at 37 °C for 72 h in 100 μl of RPMI-1640 medium containing various concentrations of the boronic acid-conjugated 4-anilinoquinazolines. After the incubation, 10 μl of 3′-(4,5-dimethylthiazol-2-yl)-2,5-diphenyltetrazolium bromide (MTT, Sigma) in PBS (5 mg/ml) was added into the each well, and the cells were further incubated at 37 °C for 4 h. After the removal of the medium, 100 μl of DMSO was added, and the absorbance at 570 nm was determined. For cell-based wash experiment,[15] A431 cells were incubated for 18 h with compounds and then washed with fresh medium. After further incubation for 54 h, the rates of viable cells were determined by MTT assay. The drug concentrations required to inhibit cell growth by 50% (GI_{50}) were determined from semilogarithmic dose–response plots.

Immunoblot analysis

After stimulation for the specified period, the cells were washed three times with PBS, dipped in 100 μl of ice-cold lysis buffer (20 mM HEPES, pH 7.4, 1% Triton-X 100, 10% glycerol, 1 mM sodium vanadate, 5 μg/ml of leupeptin, and 1 mM EDTA) for 15 min, and disrupted with a Handy Sonic Disrupter, and the lysate was boiled for 5 min in a sample buffer (50 mM Tris, pH 7.4, 4% sodium dodecylsufate (SDS), 10% glycerol, 4% 2-mercaptoethanol, and 0.05 mg/ml of bromophenol blue) at a ratio of 4:1. The proteins were separated by 10% SDS-polyacrylamide gel electrophoresis and transferred onto a PVDF membrane (Millipore). For the immunoblotting, antibodies used were phosphor-EGFR(Tyr1173) antibody (Santa Cruz), EGFR-antibody (Santa Cruz), phospho-Akt (Ser473) antibody (Cell Signaling, Beverly, MA), and phospho-p44/42 MAP kinase (Tyr204) antibody (Santa Cruz). After incubation with HRP-conjugated secondary antibody (Santa Cruz), the blot was reacted with ECL kit (GE healthcare), and the levels of each protein were visualized by a ChemiDoc XRS image analyzer (Bio-Rad).

Cell cycle analysis

After incubation of A431 cells with the drugs, the cells were washed with PBS, and fixed with 70% ethanol for 2 h at 4 °C. The cells were incubated for 30 min at 37 °C in 1 ml of RNase solution (0.25 mg/ml in PBS), and further incubated for 30 min at 4 °C in propidium iodide staining solution (PI, 0.05 mg/ml in PBS). The suspension was then passed through a 40 μm nylon mesh filter and analyzed by a Cytomics FC500 flow cytometer (Beckman Coulter).

Detection of apoptosis

Phosphatidylserine externalization was measured using an Annexin V-FITC kit (Beckman Coulter) according to the manufacturer's instructions. After incubation of A431 cells with the drugs, the cells were suspended in 100 μl of 1X binding buffer, and added 5 μl of annexin V-FITC (5 μg/ml) and 2.5 μl of PI (250 μg/ml in PBS). The cell suspensions were incubated for 10 min at 4 °C and analyzed by a flow cytometer.

Molecular docking and quantum mechanical simulations:

Docking and binding energy calculations were carried out based on the X-ray structure of EGFR kinase domain in complex with Tarceva (PDB code: 1M17).[22] Based on this structure, the entire kinase domain of the receptor protein (residues 672–964), inhibitor, and a water molecule were selected for simulations. All water molecules in the crystal structure were removed except one molecule which mediate hydrogen bond network between the protein and inhibitor (Fig. 8). Hydrogen atoms were added to the protein, considering the terminal amino acid and all charged amino acid residues the charged state. The positions of added hydrogen atoms were minimized using MMFF94x force field using the Molecular Operating Environment (MOE) software (Chemical Computing Group Inc.). The binding site of the boron-conjugated 4-anilinoquinazoline **7d** in EGFR kinase domain was defined based on that of Tarceva in the 1M17 X-ray structure. As the initial structure, the quinazoline ring of compound **7d** was superimposed on that of Tarceva retaining hydrogen bond network with the EGFR. Docking structures were calculated in two steps. First, systematic conformation search of compound **7d** in the EGFR kinase domain was performed for three rotatable bonds (Fig. 7) using the MOE software. Then two conformations were selected, in which boronic acid moiety was located at the Asp800 (model 1) or Cys797 (model 2 and model 3) interaction sites, followed by the MMFF94x minimization of the inhibitor structure at the EGFR binding site. Second, the detailed docking geometries for both Tarceva and compound **7d** were further optimized by the hybrid QM/MM simulation of quantum mechanics (QM) and molecular mechanics (MM) methods. The QM/MM calculations were carried out employing the ONIOM scheme[29,30] as implemented in GAUSSIAN03[46] using the universal force field (UFF)[47] for the MM region. The Hartree–Fock (HF) method using the 6-31G(d) basis set was chosen as the high level of theory for the QM region. The QM region consisted of side chains of Cys775, Thr790, Cys797, and Asp800, backbone of Met793, single water molecule, and the inhibitor (Fig. 8). Both side chains and backbones were capped at the Cα positions by using hydrogen link atoms, and the thiol group of Cys797 was either the –SH or the $–S^-$ form. Other residues in EGFR were treated with the UFF. With these optimized docking geometries, the binding energies between EGFR and inhibitors were calculated using the *ab initio* fragment molecular orbital (FMO) method at the HF/6-31G(d) level of theory. The FMO method is a fully QM approach and details of this method have been described elsewhere.[31–34] The approximations of electrostatic potentials considered as the Mulliken orbital charge (esp-aoc) and the fractional point charge (esp-ptc) were carried out when the distance between the closest contact atoms in the two fragments

exceed 0.0 and 2.0 in the units of van der Waals radii (vdW), respectively. In addition, the Coulomb interaction approximation (dimmer-es) was applied for the fragment pair calculations in two fragments with separations exceeding 2.0 in the same vdW unit. The fragmentation of the system was as follows: each amino acid residue of EGFR, the inhibitor molecule, and the water molecule were treated as a single fragment. All the FMO calculations were performed with the ABINIT-MP program (available at http://www.ciss.iis.u-tokyo.ac.jp/rss21/).

Acknowledgements

We thank Prof. D. Gabel (University of Bremen) for helpful discussions. KF thanks Prof. Shigenori Tanaka, Prof. Yuji Mochizuki and Dr. Tatsuya Nakano for discussions on quantum mechanical calculations. This work was supported by a Grant-in-Aid for Science Research (B) (No. 18350090) from the Ministry of Education, Culture, Sports, Science and Technology and the "Core Research for Evolutional Science and Technology" project of the Japan Science and Technology Agency (JST-CREST). Provision of computational resources from the "Revolutionary Simulation Software (RSS21)" project supported by the Ministry of Education, Culture, Sports, Science, and Technology (MEXT), Japan is gratefully acknowledged.

References

1 P. Blume-Jensen and T. Hunter, *Nature*, 2001, **411**, 355.
2 M. Dowsett, T. Cooke, I. Ellis, W. J. Gullick, B. Gusterson, E. Mallon and R. Walker, *Eur. J. Cancer*, 2000, **36**, 170.
3 H. Kim and W. J. Muller, *Exp. Cell Res.*, 1999, **253**, 78.
4 D. W. Fry, A. J. Kraker, A. McMichael, L. A. Ambroso, J. M. Nelson, W. R. Leopold, R. W. Connors and A. J. Bridges, *Science*, 1994, **265**, 1093.
5 A. E. Wakeling, S. P. Guy, J. R. Woodburn, S. E. Ashton, B. J. Curry, A. J. Barker and K. H. Gibson, *Cancer Res.*, 2002, **62**, 5749.
6 M. Fukuoka, S. Yano, G. Giaccone, T. Tamura, K. Nakagawa, J. Y. Douillard, Y. Nishiwaki, J. Vansteenkiste, S. Kudoh, D. Rischin, R. Eek, T. Horai, K. Noda, I. Takata, E. Smit, S. Averbuch, A. Macleod, A. Feyereislova, R. P. Dong and J. Baselga, *J. Clin. Oncol.*, 2003, **21**, 2237.
7 J. D. Moyer, E. G. Barbacci, K. K. Iwata, L. Arnold, B. Boman, A. Cunningham, C. DiOrio, J. Doty, M. J. Morin, M. P. Moyer, M. Neveu, V. A. Pollack, L. R. Pustilnik, M. M. Reynolds, D. Sloan, A. Theleman and P. Miller, *Cancer Res.*, 1997, **57**, 4838.
8 F. A. Shepherd, J. Rodrigues Pereira, T. Ciuleanu, E. H. Tan, V. Hirsh, S. Thongprasert, D. Campos, S. Maoleekoonpiroj, M. Smylie, R. Martins, M. van Kooten, M. Dediu, B. Findlay, D. Tu, D. Johnston, A. Bezjak, G. Clark, P. Santabarbara and L. Seymour, *N. Engl. J. Med.*, 2005, **353**, 123.
9 M. H. Nelson and C. R. Dolder, *Ann. Pharmacother.*, 2006, **40**, 261.
10 W. Xia, R. J. Mullin, B. R. Keith, L. H. Liu, H. Ma, D. W. Rusnak, G. Owens, K. J. Alligood and N. L. Spector, *Oncogene*, 2002, **21**, 6255.
11 J. A. Engelman and P. A. Janne, *Clin. Cancer Res.*, 2008, **14**, 2895.
12 E. L. Kwak, R. Sordella, D. W. Bell, N. Godin-Heymann, R. A. Okimoto, B. W. Brannigan, P. L. Harris, D. R. Driscoll, P. Fidias, T. J. Lynch, S. K. Rabindran, J. P. McGinnis, A. Wissner, S. V. Sharma, K. J. Isselbacher, J. Settleman and D. A. Haber, *Proc. Natl. Acad. Sci. U. S. A.*, 2005, **102**, 7665.
13 C. M. Discafani, M. L. Carroll, M. B. Floyd, Jr., I. J. Hollander, Z. Husain, B. D. Johnson, D. Kitchen, M. K. May, M. S. Malo, A. A. Minnick, Jr., R. Nilakantan, R. Shen, Y. F. Wang, A. Wissner and L. M. Greenberger, *Biochem. Pharmacol.*, 1999, **57**, 917.
14 D. W. Fry, A. J. Bridges, W. A. Denny, A. Doherty, K. D. Greis, J. L. Hicks, K. E. Hook, P. R. Keller, W. R. Leopold, J. A. Loo, D. J. McNamara, J. M. Nelson, V. Sherwood, J. B. Smaill, S. Trumpp-Kallmeyer and E. M. Dobrusin, *Proc. Natl. Acad. Sci. U. S. A.*, 1998, **95**, 12022.
15 H. R. Tsou, N. Mamuya, B. D. Johnson, M. F. Reich, B. C. Gruber, F. Ye, R. Nilakantan, R. Shen, C. Discafani, R. DeBlanc, R. Davis, F. E. Koehn, L. M. Greenberger, Y. F. Wang and A. Wissner, *J. Med. Chem.*, 2001, **44**, 2719.
16 C. J. Torrance, P. E. Jackson, E. Montgomery, K. W. Kinzler, B. Vogelstein, A. Wissner, M. Nunes, P. Frost and C. M. Discafani, *Nat. Med.*, 2000, **6**, 1024.
17 A. Wissner, D. M. Berger, D. H. Boschelli, M. B. Floyd, Jr., L. M. Greenberger, B. C. Gruber, B. D. Johnson, N. Mamuya, R. Nilakantan, M. F. Reich, R. Shen, H. R. Tsou, E. Upeslacis, Y. F. Wang, B. Wu, F. Ye and N. Zhang, *J. Med. Chem.*, 2000, **43**, 3244.
18 S. K. Rabindran, C. M. Discafani, E. C. Rosfjord, M. Baxter, M. B. Floyd, J. Golas, W. A. Hallett, B. D. Johnson, R. Nilakantan, E. Overbeek, M. F. Reich, R. Shen, X. Shi, H. R. Tsou, Y. F. Wang and A. Wissner, *Cancer Res.*, 2004, **64**, 3958.
19 J. M. Nelson and D. W. Fry, *J. Biol. Chem.*, 2001, **276**, 14842.
20 J. B. Smaill, G. W. Rewcastle, J. A. Loo, K. D. Greis, O. H. Chan, E. L. Reyner, E. Lipka, H. D. Showalter, P. W. Vincent, W. L. Elliott and W. A. Denny, *J. Med. Chem.*, 2000, **43**, 3199.
21 J. A. Blair, D. Rauh, C. Kung, C. H. Yun, Q. W. Fan, H. Rode, C. Zhang, M. J. Eck, W. A. Weiss and K. M. Shokat, *Nat. Chem. Biol.*, 2007, **3**, 229.
22 J. Stamos, M. X. Sliwkowski and C. Eigenbrot, *J. Biol. Chem.*, 2002, **277**, 46265.
23 M. Groll, C. R. Berkers, H. L. Ploegh and H. Ovaa, *Structure*, 2006, **14**, 451.
24 F. A. Cotton, G. Wilkinson and P. L. Gaus, *Basic Inorganic Chemistry*, Wiley, New York, 1987, p. 7.
25 P. R. Rablen, *J. Am. Chem. Soc.*, 1997, **119**, 8350.
26 F. A. Cotton, G. Wilkinson and P. L. Gaus, *Basic Inorganic Chemistry*, Wiley, New York, 1987, p. 257.
27 A. F. Kisselev and A. L. Goldberg, *Chem. Biol.*, 2001, **8**, 739.
28 K. Raha, M. B. Peters, B. Wang, N. Yu, A. M. Wollacott, L. M. Westerhoff and K. M. Merz, Jr., *Drug Discovery Today*, 2007, **12**, 725.
29 F. Maseras and K. Morokuma, *J. Comput. Chem.*, 1995, **16**, 1170.
30 T. Vreven, K. S. Byun, I. Komaromi, S. Dapprich, Montgomery, A. John, K. Morokuma and M. J. Frisch, *J. Chem. Theory Comput.*, 2006, **2**, 815.
31 K. Kitaura, T. Sawai, T. Asada, T. Nakano and M. Uebayasi, *Chem. Phys. Lett.*, 1999, **312**, 319.
32 K. Kitaura, E. Ikeo, T. Asada, T. Nakano and M. Uebayasi, *Chem. Phys. Lett.*, 1999, **313**, 701.
33 T. Nakano, T. Kaminuma, T. Sato, Y. Akiyama, M. Uebayasi and K. Kitaura, *Chem. Phys. Lett.*, 2000, **318**, 614.
34 T. Nakano, T. Kaminuma, T. Sato, K. Fukuzawa, Y. Akiyama, M. Uebayasi and K. Kitaura, *Chem. Phys. Lett.*, 2002, **351**, 475.
35 K. Fukuzawa, K. Kitaura, M. Uebayasi, K. Nakata, T. Kaminuma and T. Nakano, *J. Comput. Chem.*, 2005, **26**, 1.
36 K. Fukuzawa, Y. Mochizuki, S. Tanaka, K. Kitaura and T. Nakano, *J. Phys. Chem. B*, 2006, **110**, 16102.
37 J. A. Grosso, D. E. Nichols, J. D. Kohli and D. Glock, *J. Med. Chem.*, 1982, **25**, 703.
38 A. J. Bridges, H. Zhou, D. R. Cody, G. W. Rewcastle, A. McMichael, H. D. Showalter, D. W. Fry, A. J. Kraker and W. A. Denny, *J. Med. Chem.*, 1996, **39**, 267.
39 T. J. Michnick and D. S. Matteson, *Synlett*, 1991, 631.
40 G. A. Molander, C.-S. Yun, M. Ribagorda and B. Biolatto, *J. Org. Chem.*, 2003, **68**, 5534.
41 E. G. Barbacci, L. R. Pustilnik, A. M. Rossi, E. Emerson, P. E. Miller, B. P. Boscoe, E. D. Cox, K. K. Iwata, J. P. Jani, K. Provoncha, J. C. Kath, Z. Liu and J. D. Moyer, *Cancer Res.*, 2003, **63**, 4450.
42 J. S. Sebolt-Leopold and J. M. English, *Nature*, 2006, **441**, 457.
43 H. Nakamura, H. Kuroda, H. Saito, R. Suzuki, T. Yamori, K. Maruyama and T. Haga, *ChemMedChem*, 2006, **1**, 729.
44 S. J. Decker, C. Alexander and T. Habib, *J. Biol. Chem.*, 1992, **267**, 1104.
45 J. Singh, E. M. Dobrusin, D. W. Fry, T. Haske, A. Whitty and D. J. McNamara, *J. Med. Chem.*, 1997, **40**, 1130.
46 M. J. T. Frisch, , H. B. Schlegel, G. E. Scuseria, M. A. Robb, J. R. Cheeseman, J. A. Montgomery, Jr., T. Vreven, K. N. Kudin, J. C. Burant, J. M. Millam, S. S. Iyengar, J. Tomasi, V. Barone, B. Mennucci, M. Cossi, G. Scalmani, N. Rega, G. A. Petersson, H. Nakatsuji, M. Hada, M. Ehara, K. Toyota, R. Fukuda, J. Hasegawa, M. Ishida, T. Nakajima, Y. Honda, O. Kitao, H. Nakai, M. Klene, X. Li, J. E. Knox, H. P. Hratchian, J. B. Cross, V. Bakken, C. Adamo, J. Jaramillo,

R. Gomperts, R. E. Stratmann, O. Yazyev, A. J. Austin, R. Cammi, C. Pomelli, J. W. Ochterski, P. Y. Ayala, K. Morokuma, G. A. Voth, P. Salvador, J. J. Dannenberg, V. G. Zakrzewski, S. Dapprich, A. D. Daniels, M. C. Strain, O. Farkas, D. K. Malick, A. D. Rabuck, K. Raghavachari, J. B. Foresman, J. V. Ortiz, Q. Cui, A. G. Baboul, S. Clifford, J. Cioslowski, B. B. Stefanov, G. Liu, A. Liashenko, P. Piskorz, I. Komaromi, R. L. Martin, D. J. Fox, T. Keith, M. A. Al-Laham, C. Y. Peng, A. Nanayakkara, M. Challacombe, P. M. W. Gill, B. Johnson, W. Chen, M. W. Wong, C. Gonzalez and J. A. Pople, *Gaussian 03, Revision C.02*, Gaussian, Inc., Wallingford CT, 2004.

47 A. K. Rappe, C. J. Casewit, K. S. Colwell, W. A. Goddard and W. M. Skiff, *J. Am. Chem. Soc.*, 1992, **114**, 10024.